

Deformação por Maclação e Transformações Martensíticas

Maclas e Placas de Martensita

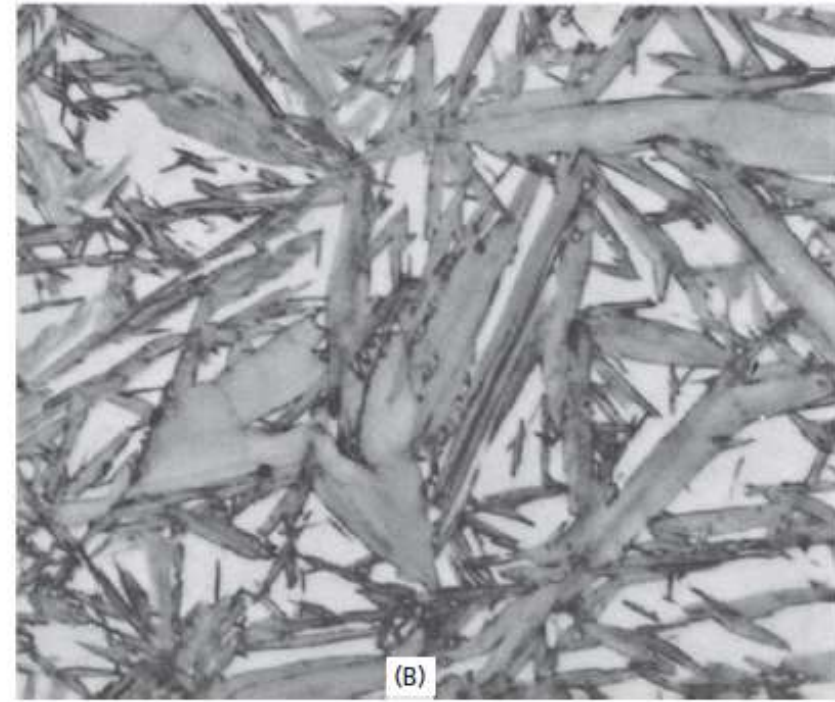
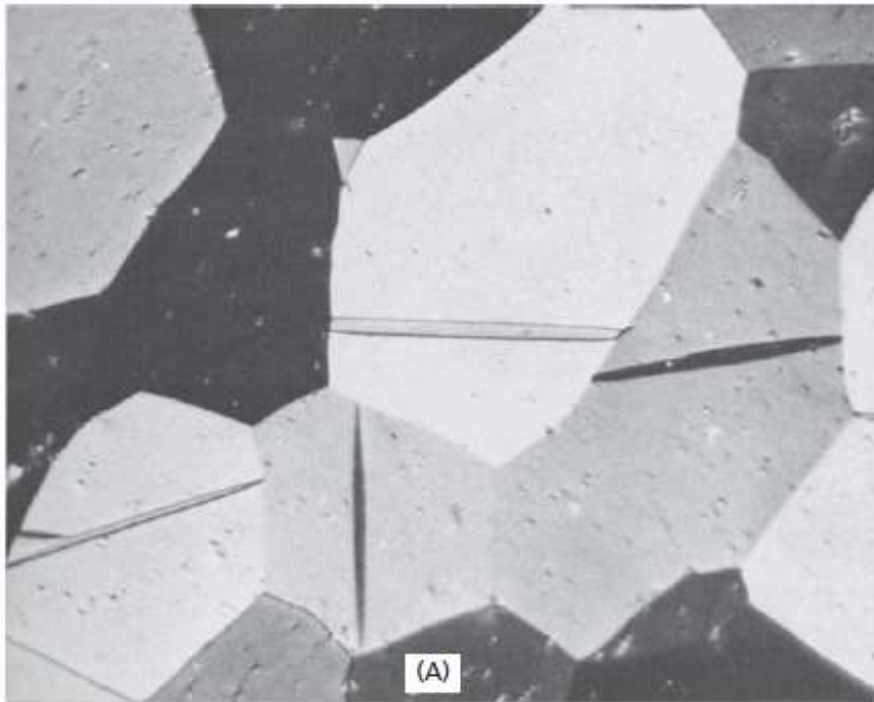


FIG. 17.1 (A) Deformation twins in a polycrystalline zirconium specimen. Photographed with polarized light. (E. R. Buchanan.) 1500 \times . (B) Martensite plates in a 1.5 percent carbon-5.10 percent nickel steel. (Courtesy of E. C. Bain Laboratory for Fundamental Research, United States Steel Corporation.) 2500 \times

Macla

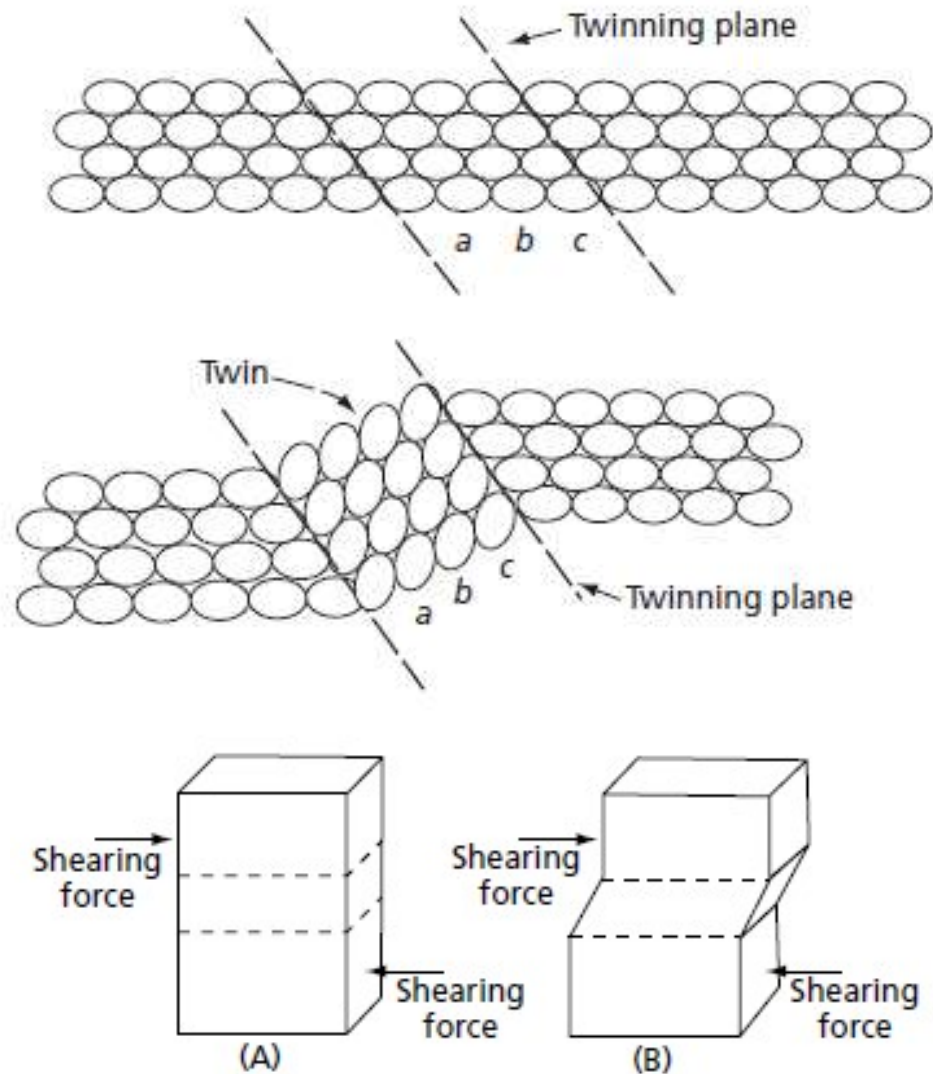


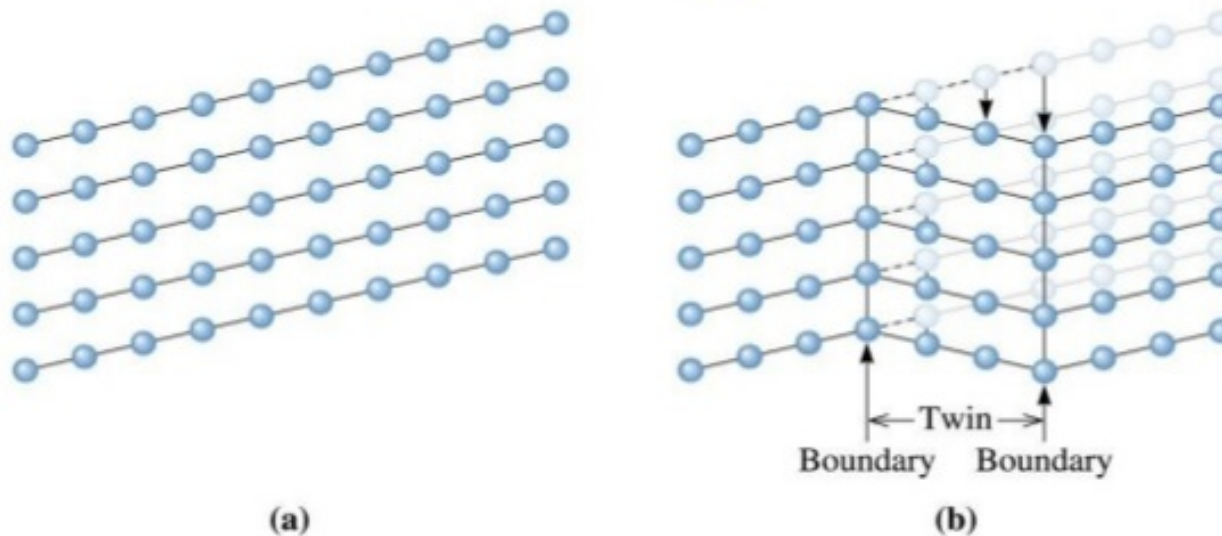
FIG. 17.3 Schematic representation showing how a twin may be produced by a simple movement of atoms

FIG. 17.4 (A) shows a single crystal in a position where it is subject to shearing forces. (B) shows a twinning shear that has occurred as a result of the force

Maclação de cristais

- Formação de maclas por deformação

Twinning



Applied stress to a perfect crystal (a) may cause a displacement of the atoms, (b) causing the formation of a twin. Note that the crystal has deformed as a result of twinning.



Tipos de Maclas

It follows from the above that there are three ways that a crystal lattice can be sheared while still retaining its crystal structure and symmetry:

1. When K_1 is a rational plane and η_2 a rational direction. (A twin of the first kind)
2. When K_2 is a rational plane and η_1 a rational direction. (A twin of the second kind)
3. When all four elements K_1 , K_2 , η_1 , and η_2 are rational. (A compound twin)

K_1 = the twinning plane, or the first undistorted plane

K_2 = the second undistorted plane

η_1 = the shear direction

η_2 = the direction defined by the intersection of the plane of shear with K_2

Tipos de maclas

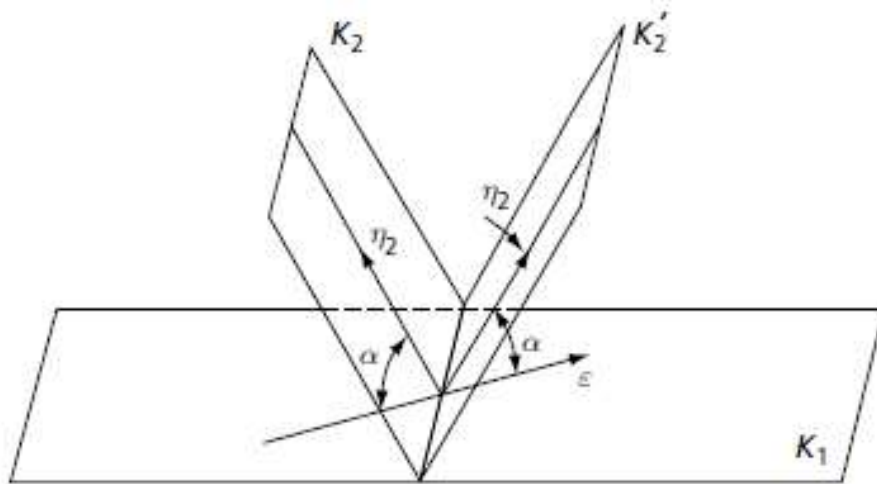


FIG. 17.8 In this figure, which corresponds to a shear of the first kind, notice that η_2 makes equal angles with an arbitrary vector ε , which lies in K_1 , both before and after the shear. The sheared position of the second undistorted plane is designated K'_2

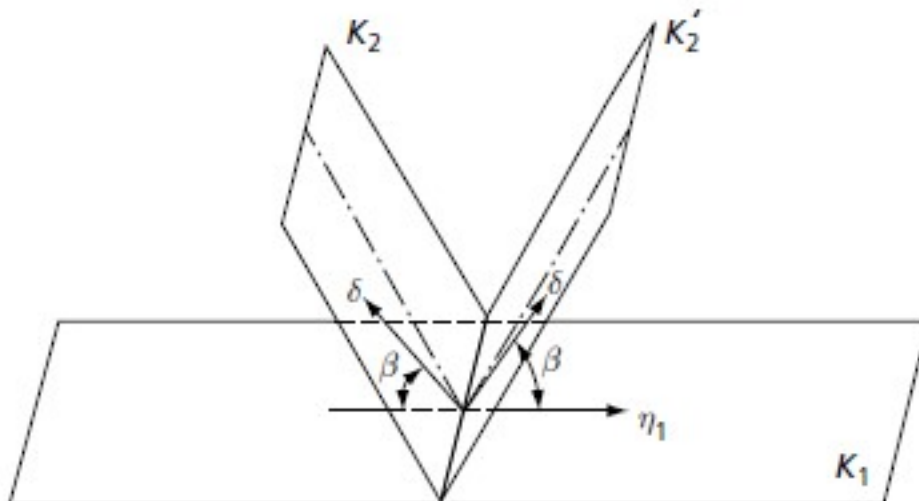


FIG. 17.9 This diagram represents a shear of the second kind. In this case δ represents an arbitrary vector in K_2 which makes the same angle with η_1 before and after shearing. The sheared position of the second undistorted plane is designated K'_2

Contorno de Macla

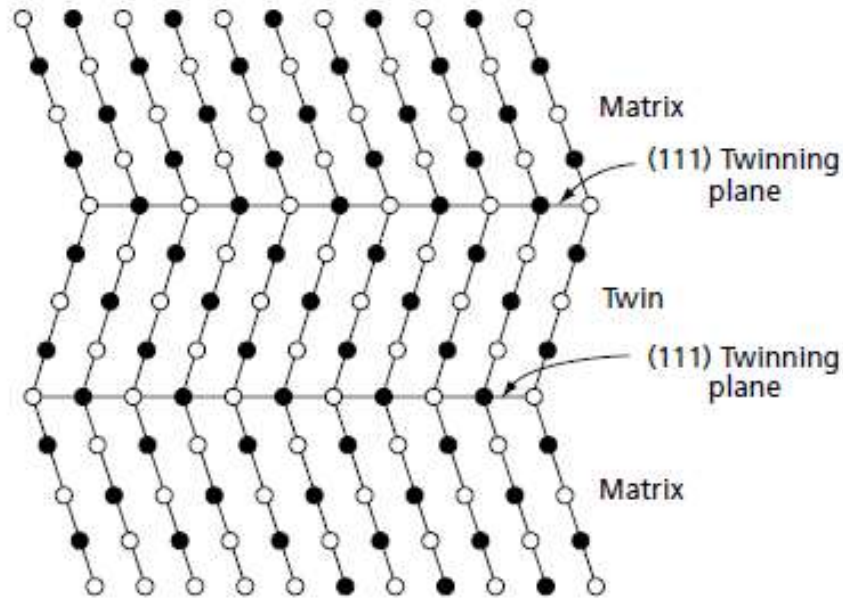


FIG. 17.15 Atomic arrangement at the twinning plane in a face-centered cubic metal. Black and white circles represent atoms on different levels (planes). (After Barrett, C. S., ASM Seminar, *Cold Working of Metals*, 1949, Cleveland, Ohio, p. 65.)

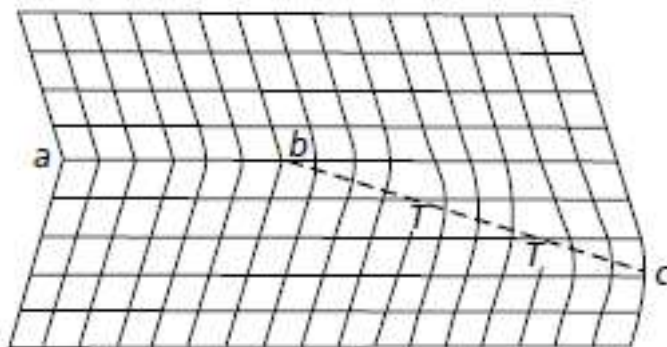


FIG. 17.16 The difference between a coherent twin boundary ab and an incoherent twin boundary bc . Notice the dislocations in the incoherent boundary. (After Siems, R., and Haasen, P., *Zeits. für Metallkunde*, **49** 213 [1958].)

Deformação por maclação

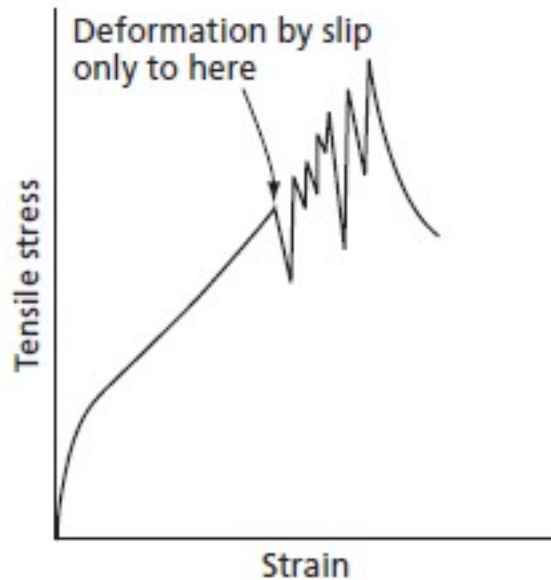


FIG. 17.18 Single-crystal tensile stress-strain curve showing discontinuous strain increments due to twinning. (After Schmid and Boas, *Kristallplastizität*, Julius Springer, Berlin, 1935.)

Deformação por maclação

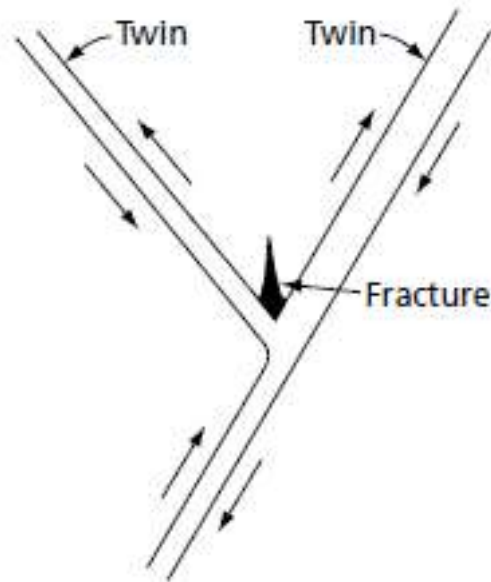


FIG. 17.19 A crack induced in an iron crystal at a twin intersection. Similar cracks were first reported by Rose in 1868. (After Priestner, R., *Deformation Twinning*, AIME Conf. Series, vol. 25, p. 321, Gordon and Breach Science Publishers, New York, 1964.)

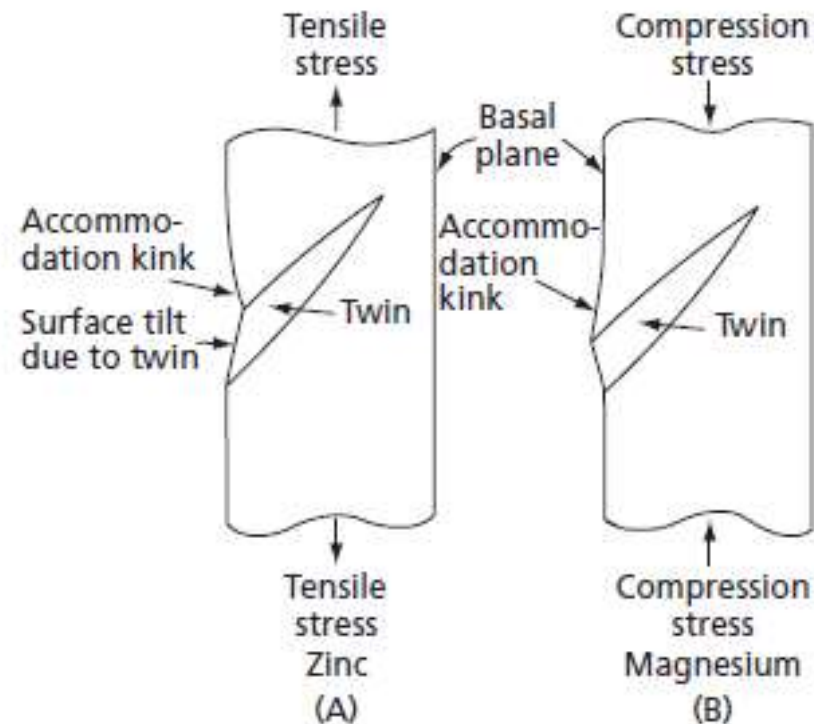


FIG. 17.20 Surface tilts and accommodation kinks resulting from intersections of half-lens twins with the surface in two hexagonal metals

Martensita – distorção de Bain

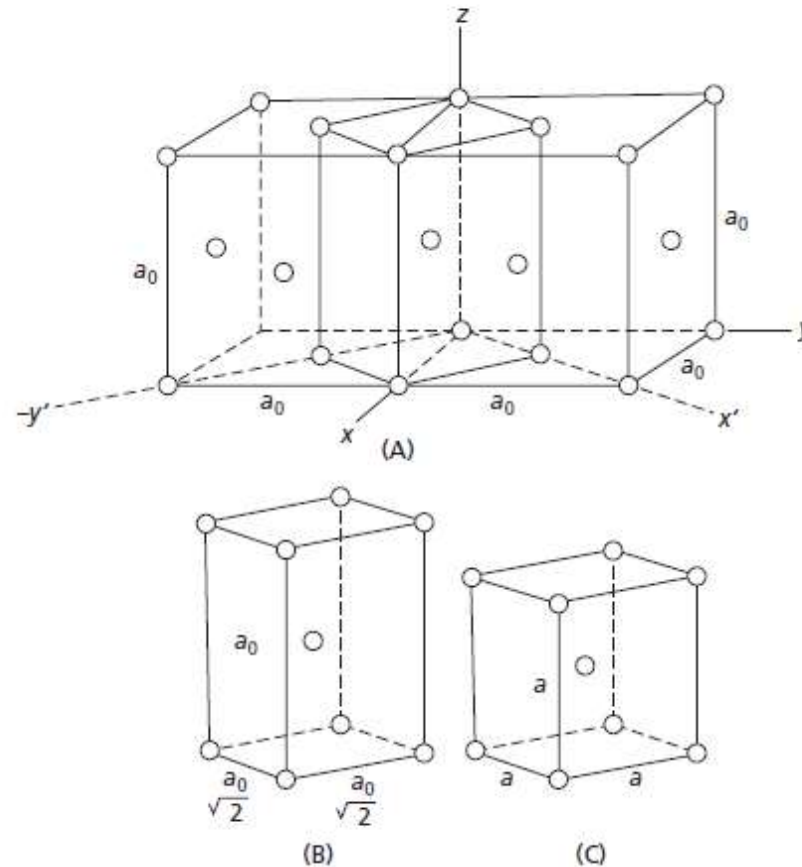
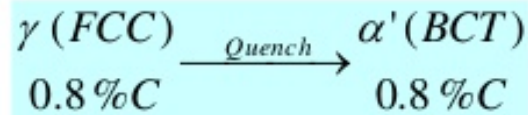


FIG. 17.22 Bain distortion for a face-centered cubic lattice transforming to a body-centered cubic lattice. The body-centered tetragonal cell is outlined in the face-centered cubic structure in (A), and shown alone in (B). The Bain distortion converts (B) to (C). (After Wechsler, M. S., Lieberman, D. S., and Read, T. A., *Trans. AIME*, **197** 1503 [1953].)

Transformação Martensítica

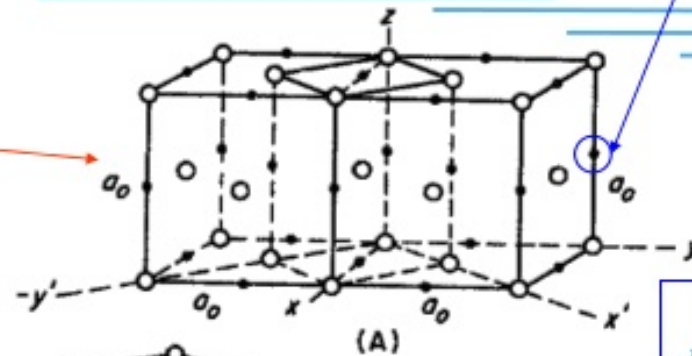
Martensite



Possible positions of Carbon atoms

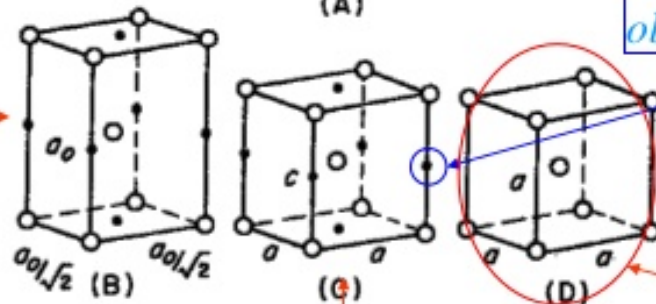
Only a fraction of the sites occupied

FCC Austenite



C along the c-axis obstructs the contraction

FCC Austenite
Alternate choice of Cell

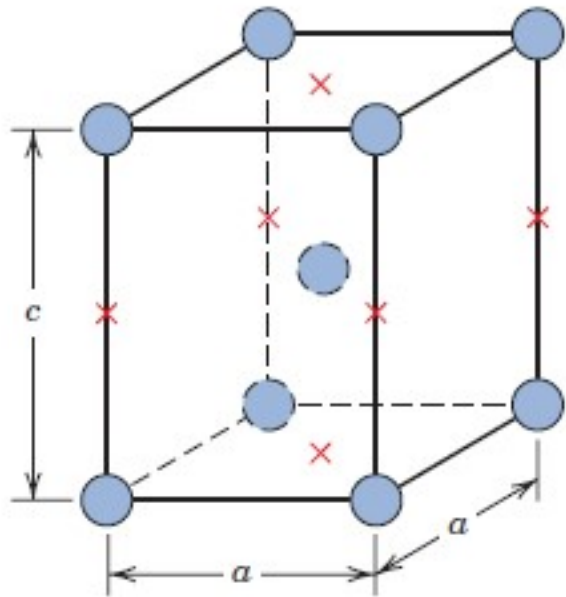


20% contraction of *c*-axis
12% expansion of *a*-axis

Tetragonal Martensite

In Pure Fe after the Martensitic transformation
 $c = a$

Martensita



Placas de martensita em meia à austenita

Histerese

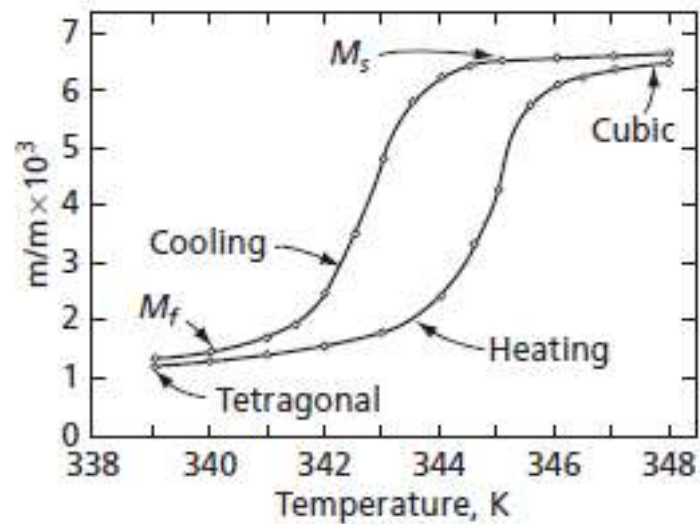


FIG. 17.24 The temperature dependence of the martensite transformation in the indium-thallium (18 percent TI) alloy. Transformation followed by measurement of change in length of specimen. (From data of Burkart, M. W., and Read, T. A., *Trans. AIME*, **197** 1516 [1953].)

Transformação atérmica

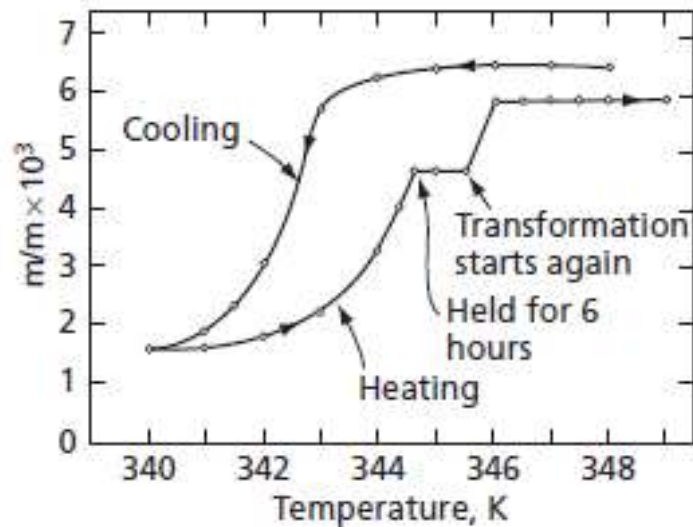


FIG. 17.25 Stabilization in the martensite transformation in an indium-thallium (18 percent Tl) alloy. (From data of Burkart, M. W., and Read, T. A., *Trans AIME*, 197 1516 [1953].)

Formação das placas de martensita

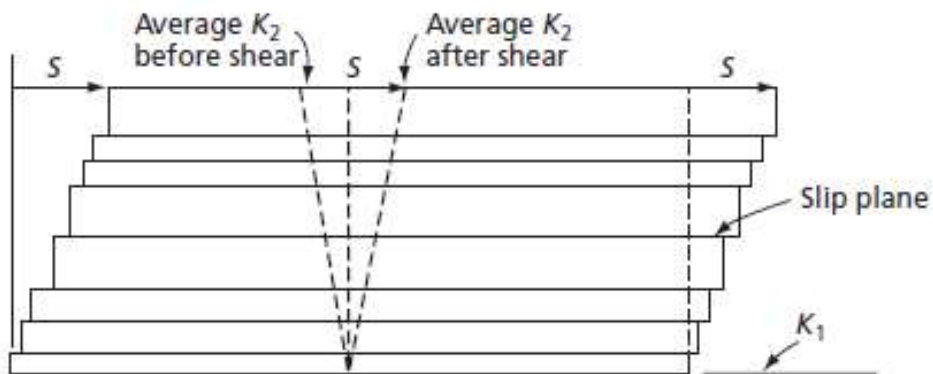


FIG. 17.30 Martensitic shear assuming that deformation occurs by slip

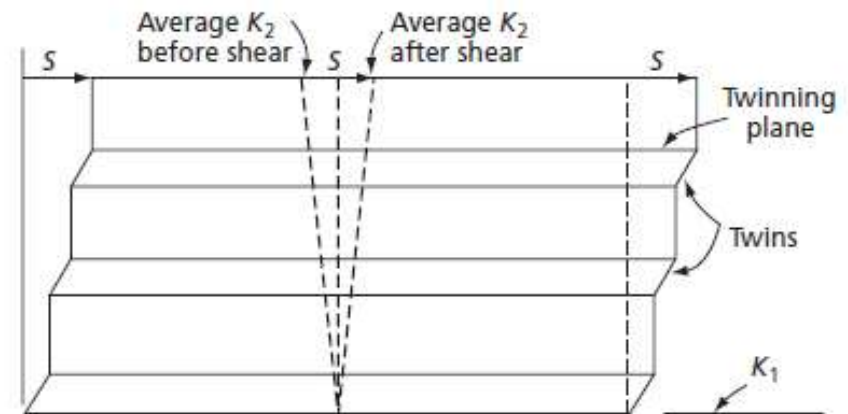


FIG. 17.31 Martensitic shear assuming that deformation occurs by deformation twinning. The required shear is met when only a fraction of the structure twins in a series of bands parallel to the twinning plane

Formação das placas de martensita

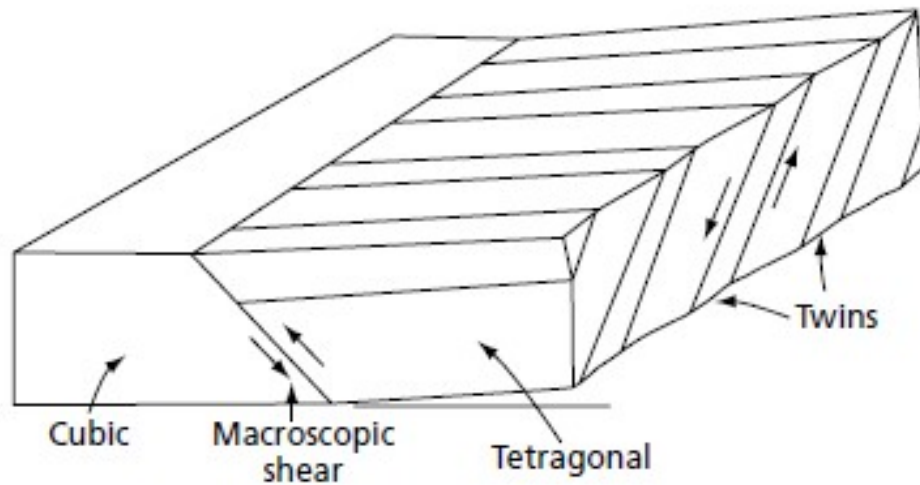
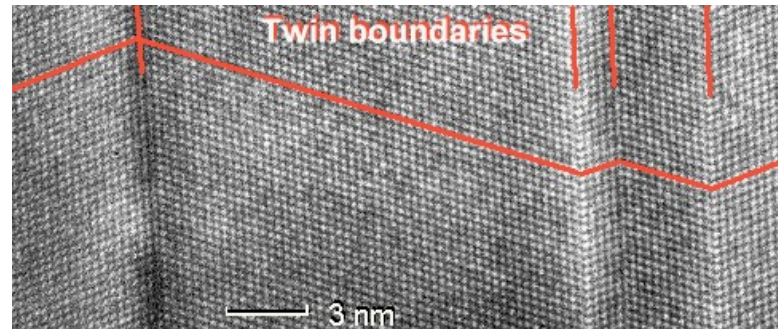
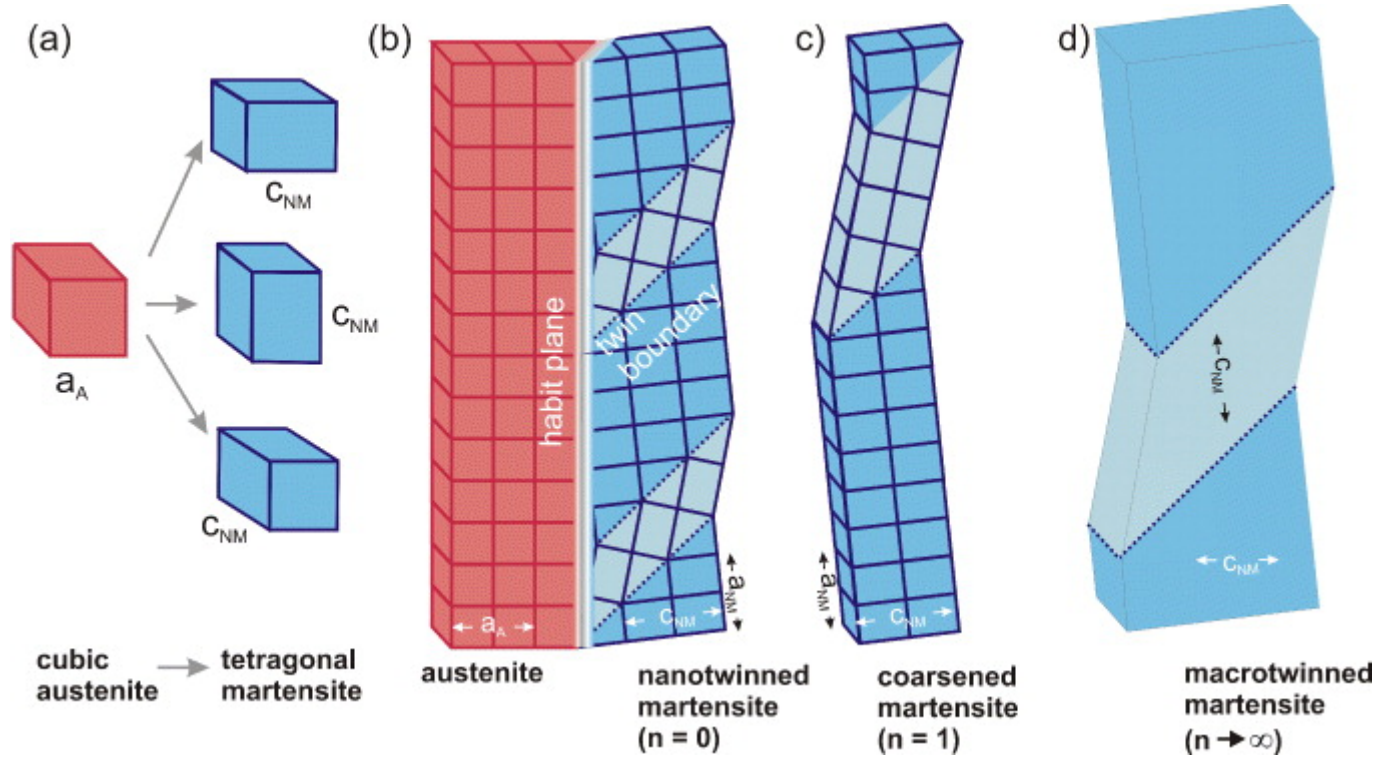


FIG. 17.32 The nature of the twinned tetragonal structure in the indium-thallium martensite transformation

Martensita maclada



Transformação induzida por tensão

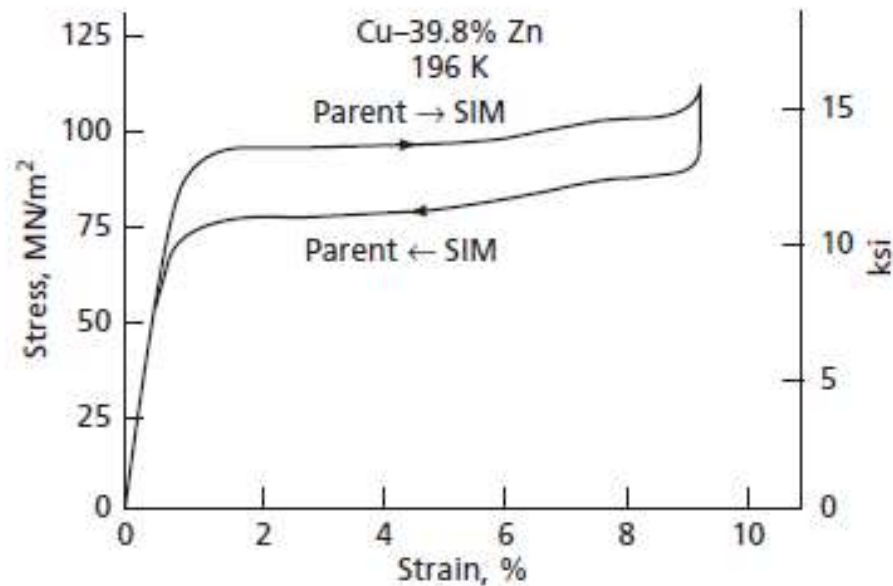


FIG. 17.39 A stress-strain curve loop resulting from loading and unloading a superelastic alloy above M_s . (Reprinted from *Acta Metallurgica*, 27, Schroeder, T.A., and Wayman, C.M., Pseudoelastic effects in Cu-Zn single crystals, 405, Copyright 1979, with permission from Elsevier. <http://www.sciencedirect.com/science/journal/00016160>)

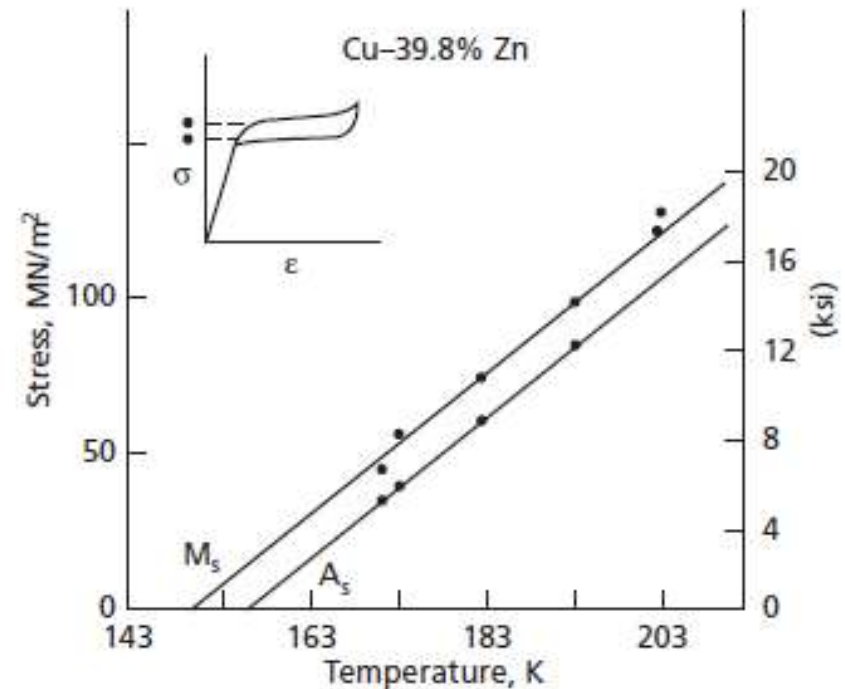


FIG. 17.40 Temperature dependence of the stresses at M_s and A_s . (Reprinted from *Acta Metallurgica*, 27, Schroeder, T.A., and Wayman, C.M., Pseudoelastic effects in Cu Zn single crystals, 405, Copyright 1979, with permission from Elsevier. <http://www.sciencedirect.com/science/journal/00016160>)

Efeito de memória de forma

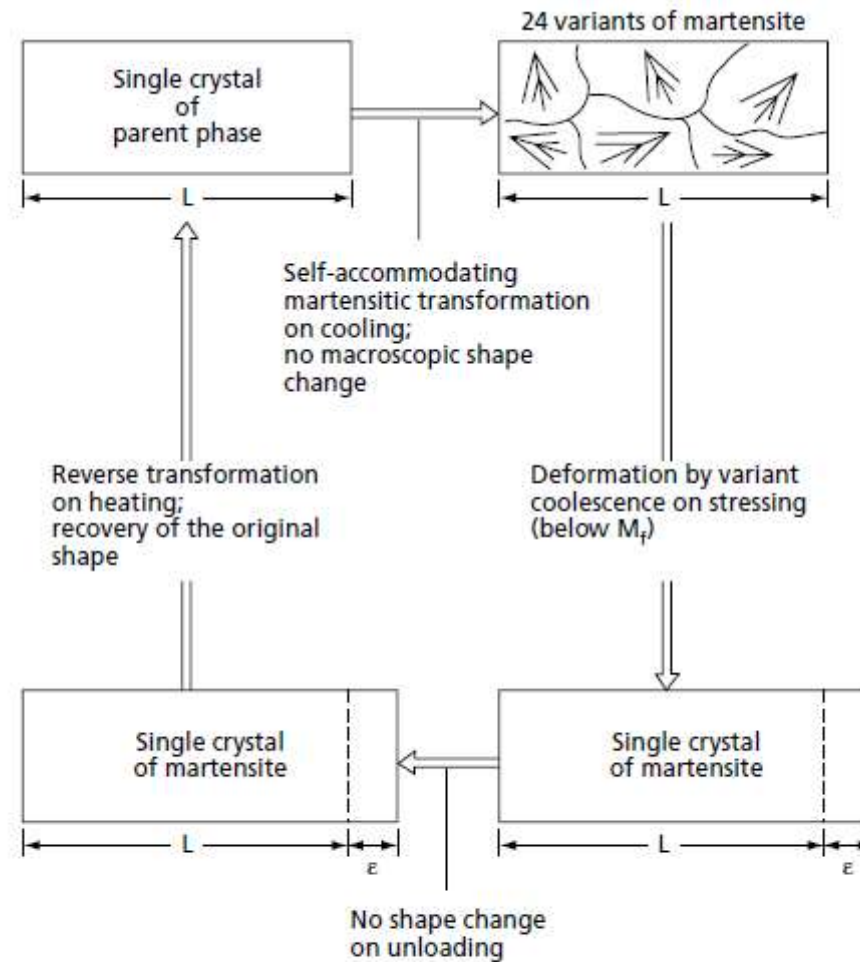
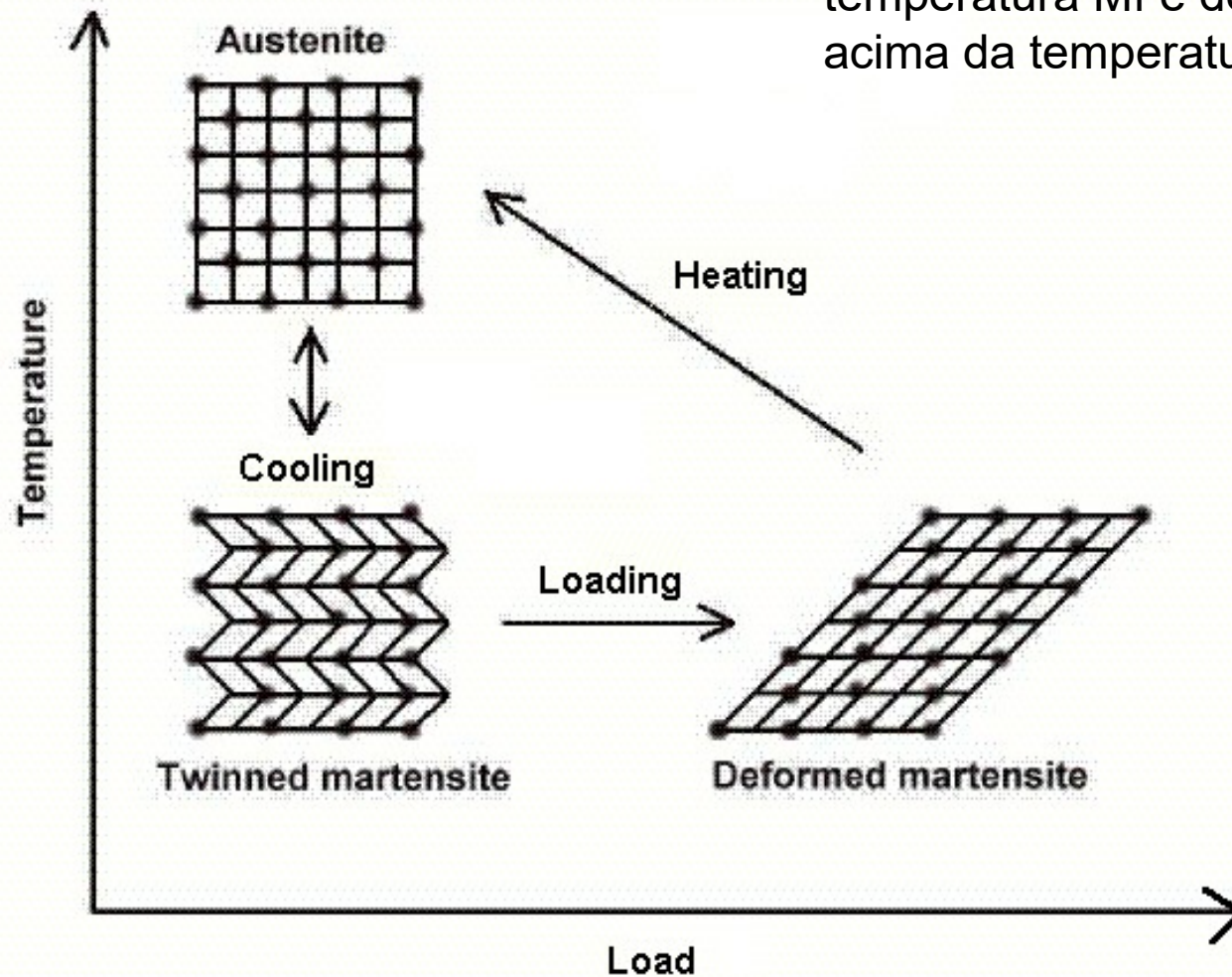


FIG. 17.42 A schematic diagram illustrating the shape-memory processes. (From Wayman, C. M., *Solid \rightarrow Solid Phase Transformations*, Aaronson, H. I., Loughin, D. E., Sekerka, R. F., and Wayman, C. M., Eds., p. 1138, *Met. Soc. AIME*, Warrendale, Pa., 1981 p. 1138, Figure 12.)

Efeito de memória de forma

Quando a liga é deformada abaixo da temperatura M_f e depois aquecida acima da temperatura A_f



Superelasticidade (pseudo-elasticidade)

